Journal of Sustainable Metallurgy (2021) 7:1469–1482
https://doi.org/10.1007/s40831-021-00442-3

THEMATIC SECTION: MINE TAILINGS: PROBLEM OR OPPORTUNITY? TOWARDS A COMBINED REMEDIATION AND RESOURCE RECOVERY APPROACH

Turning Mine Waste into a Ceramic Resource: Plombières Tailing Case

Francisco Veiga Simão[1,2,3] · Hilde Chambart[1] · Laure Vandemeulebroeke[1] · Peter Nielsen[4] · Valérie Cappuyns[2,3]

Received: 28 May 2021 / Accepted: 13 September 2021 / Published online: 18 October 2021

Abstract

Mining and quarrying waste is the second largest waste stream in Europe. Sulfidic ore processing residues (tailings) pose a large challenge, because they contain hazardous metal(loid)s and because they can lead to acid mine drainage. However, mine tailings also contain valuable base, precious, and critical metals, which can be used in different technological applications, as well as silicates and clay minerals that offer possibilities for use in building materials. In the present study, the potential use of mine tailing material, from the inactive Pb–Zn mine of Plombières (Eastern Belgium), in three ceramic products (roof tiles, blocks, and pavers) was assessed, taking into account production parameters, product quality, and environmental performance. After a detailed physical, mineralogical, and chemical characterization of the mine tailing material and the original raw materials, different mixtures were prepared on a lab scale, in which primary raw materials (e.g., clay and sand) were replaced by 5, 10, or 20 wt% of the fine tailing material. The technical, chemical, and aesthetical properties of each ceramic body were assessed, as well as their environmental performance, considering a 2nd life scenario, where shaped building materials are demolished and recycled as aggregates. High additions of tailing material in clay roof tiles (10 and 20 wt%) and clay blocks (20 wt%) resulted in technical and aesthetical problems. On the contrary, paver mixtures containing 10 and 20 wt% of tailing material showed better technical properties and satisfying chemical and aesthetical characteristics.

The contributing editor for this article was Mirja Illikainen

✉ Francisco Veiga Simão
francisco.veiga@kuleuven.be

Hilde Chambart
hilde.chambart@wienerberger.com

Laure Vandemeulebroeke
laure.vandemeulebroeke@wienerberger.com

Peter Nielsen
peter.nielsen@vito.be

Valérie Cappuyns
valerie.cappuyns@kuleuven.be

[1] Central Laboratory for Clay Roof Tiles, Wienerberger NV, Kapel ter Bede 121, 8500 Kortrijk, Belgium

[2] Research Centre for Economics and Corporate Sustainability, KU Leuven, Warmoesberg 26, 1000 Brussels, Belgium

[3] Division of Geology, Department of Earth and Environmental Sciences, KU Leuven, Celestijnenlaan 200E, 3001 Leuven, Belgium

[4] Laboratory of Waste and Recycling Technologies, Sustainable Materials Unit, VITO NV, Boeretang 200, 2400 Mol, Belgium

Graphical Abstract

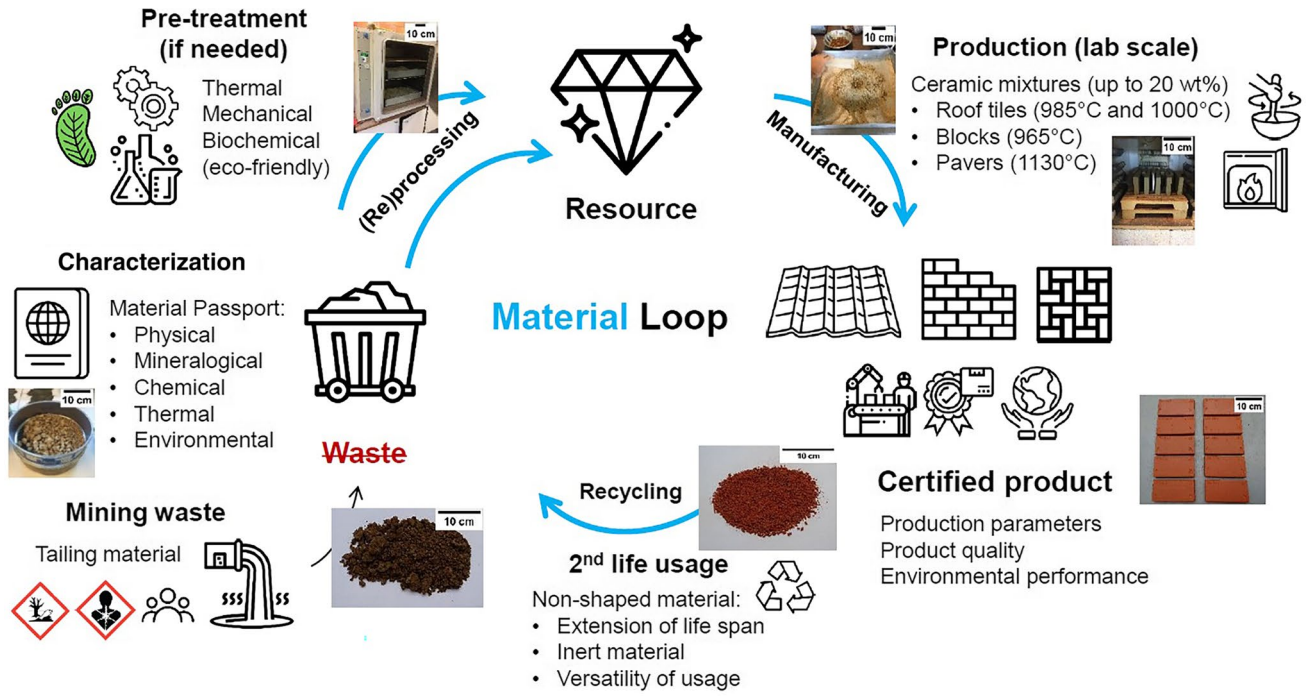

Keywords Plombières tailing · Valorization · Ceramics · Clay roof tiles · Clay blocks · Clay pavers

Introduction

Mining waste is considered one of the world's largest industrial waste streams [1]. It is defined as the high-volume material that originates from the processes of excavation, dressing, and further physical and chemical processing of a wide range of metalliferous and non-metalliferous minerals [2]. During the excavation of the mineral ore, topsoil, overburden, and waste rock are generated, while during the processing of the mineral ore, tailings and other processing waste (e.g., slurry) are generated [3]. Acid-generating tailings from processing sulfide ores are classified as hazardous waste according to the European List of Waste [4]. They pose a large challenge as they can lead to acid mine drainage (AMD). After the main ore processing steps of crushing, grinding, milling, and chemical leaching, metal(loid)s and sulfur from sulfidic mine tailings tend to become more chemically available, resulting in the potential generation of AMD [5]. AMD can cause environmental and health hazards, and social prejudice to the nearby population [6]. Additionally, mismanagement of (sulfidic) tailing ponds can turn into catastrophic events, such as the recent Brumadinho tailings pond collapse [7]. Moreover, the finer particle size of tailings can affect visual and respiratory systems in humans and animals, as well as damage crops in nearby areas [8, 9]. Additionally, high costs are associated with the disposal of mine tailings and with the restoration of affected areas.

The incorporation of mining and quarrying waste from extraction or processing steps, not including metallurgical or other industrial waste, in traditional ceramics, such as ceramic bricks, has been broadly studied and described in review articles [10–14]. Ceramic roof tiles, blocks, and pavers are less frequently considered. Only a few studies address the use of mining waste materials in *ceramic roof tiles*. The combination of kaolin processing waste and granite sawing dust (up to 50 wt%) in ceramic roof tile mixtures showed better mechanical properties at lower sintering temperatures when compared to the use of kaolin processing waste only [15]. Hard rock waste from blasting and crushing processes mixed with red clay (up to 40 wt%) has shown satisfying technical properties (water absorption and mechanical strength), which makes it a good alternative material for use in ceramic roof tiles, without the need of further glazing [16]. Initial tests using Au–Ag tailings (up to 55 wt%) in clay mixtures for the production of roof tiles have shown satisfying grain size distribution and natural colors [17]. Replacement of raw materials by mining waste, such as kaolin processing waste and granite sawing dust (up to 50 wt%), in *ceramic blocks* did not change technical and mechanical properties [15, 18].

Waste clay from coal preparation tailings mixed with primary clay (up to 15 wt%) showed acceptable mechanical and chemical properties at higher firing temperatures for ceramic blocks [19]. Ornamental rock waste mixed with clay showed satisfying physical and chemical results for the manufacturing of ceramic blocks [20]. Regarding the use of mining waste in *ceramic pavers*, a study with ornamental rock waste, mixed with yellow clay, was done [21]. The ceramic pavers showed an increase in dry density, better sintering at higher temperatures, as well as decreasing water absorption levels. Other recent studies dealing with mine waste [22] and industrial waste [23–25] application in ceramics showed satisfactory results for these alternative materials.

A previous study [26] showed that mine tailings from Plombières (Belgium) proved to be a good fit to partly or totally replace some of the primary raw materials (mainly clay and sand) in ceramic roof tiles (5 wt%) and blocks (10 wt%), taking into account production parameters and product quality standards. The aim of the present study is to assess the incorporation of higher amounts (up to 20 wt%) of the same tailing material in 3 different ceramic products (roof tiles, blocks, and pavers), having different compositions and firing temperatures. Production parameters (shaping, drying, and firing), product quality (technical, chemical, and aesthetical properties), and environmental performance (2nd life scenario) of the ceramic products were assessed.

Materials

Mining Waste

At the former Pb–Zn mining site of Plombières (Eastern Belgium), inactive since 1922 [27], around 11.4 Mt of mine waste is stored in tailing ponds covered with soils and metallurgical waste [28]. This mining waste consists of dumped material from the mining operations. It contains red to black iron oxides, coal-rich black material, slag material, ash, Zn–Pb mining waste, ceramic pipes, old ceramic bricks, and clay mixed with fine-grained dolomite ($CaMg(CO_3)_2$) sand as a mineral dressing waste [29]. For this study, a tailing sample (SUL_PL_62_I) from a selected tailing pond layer was sampled at 1.10 m of depth, through a hand-excavated pit hole. This selected layer is a Pb–Zn-poor yellow tailing material considered as the most prominent layer in the studied tailing pond, with an estimated quantity of 32,000 t (on a total of 44,000 t) [30]. The first meter of heterogeneous material was removed in order to gain access to the yellow tailing material (SUL_PL_62_I). About 25 kg of the material was sampled and stored in sealed containers.

Clay Roof Tiles

For the production of clay roof tile test specimens, one company-specific blend (PM) was selected, composed of three different primary raw materials (local clay, local sand, and imported clay), and one secondary raw material (imported filler G), which is a by-product from another industrial activity. Local raw materials (clay and sand) were collected from the quarries, while the imported clay and filler were sampled at the production plant. The selected clay roof tile blend was modified on lab scale, by partly replacing two primary raw materials (local clay and sand) by 5 wt% and 10 wt% of tailing material (SUL_PL_62_I). In the roof tile blend with 20 wt% addition of tailing material, all four original composing raw materials were partly replaced (Table 1).

Clay Inner-Wall Blocks

For the production of clay inner-wall blocks, one company-specific blend (ZM) was selected, containing five different primary raw materials (local clay, regional sand, regional filler, imported filler B, and imported filler R), and one waste material (imported waste), which is an industrial by-product. Local clay was collected from the quarry, and all the other materials were sampled at the production plant. The selected block blend was modified on lab scale. In the blend with 10 wt% tailing material, the sand was completely replaced, while filler R was partly replaced. For the block blend with the highest addition of tailing material (20 wt%), apart from the replaced sand and partly replaced filler R, the local clay was also partly replaced (Table 1).

Clay Pavers

For the production of clay pavers, one company-specific blend (KM) was selected. The ready-for-use mixture was sampled at the production plant and modified in the lab by replacing 10 and 20 wt% of the mixture by tailing material (Table 1).

Methods

Pre-treatment of Samples

All samples were dried overnight in a ventilated drying stove (Heraeus UT 6060) at 105 °C. Once dried, the local clay, imported clay, and paver mix were ground using a shredding machine (Hosokawa-Alpine MZ-25) in order to facilitate the integration in the ceramic mixtures. This process did not change the original grain size distribution of the samples. The three fillers (regional filler, imported filler R, and imported filler B) from the block blend were ground, using

Table 1 Composition of clay roof tile (A), block (B), and paver (C) mixtures on dry weight basis

A. Roof tile mix	Local clay (wt%)	Local sand (wt%)	Imported clay (wt%)	Imported filler G (wt%)	Additive ($BaCO_3$) (wt%)	SUL_PL_62_I (wt%)	Total[a] (wt%)
SUL_PM_1	31.0	28.0	24.0	17.0	0.5	0.0	100.5
SUL_PM_2	27.0	27.0	24.0	17.0	0.5	5.0	100.5
SUL_PM_3	23.0	26.0	24.0	17.0	0.5	10.0	100.5
SUL_PM_4	21.0	24.0	20.0	15.0	0.5	20.0	100.5

B. Block mix	Local clay (wt%)	Imported filler B (wt%)	Regional filler (wt%)	Imported filler R (wt%)	Imported waste (wt%)	Regional sand (wt%)	SUL_PL_62_I (wt%)	Total (wt%)
SUL_ZM_1	44.8	19.3	16.6	11.4	2.3	5.6	0.0	100.0
SUL_ZM_2	44.8	19.3	16.6	7.0	2.3	0.0	10.0	100.0
SUL_ZM_3	36.8	19.3	16.6	5.0	2.3	0.0	20.0	100.0

C. Paver mix	Paver mix (wt%)	SUL_PL_62_I (wt%)	Total (wt%)
SUL_KM_1	100.0	0.0	100.0
SUL_KM_2	90.0	10.0	100.0
SUL_KM_3	80.0	20.0	100.0

[a]$BaCO_3$ (0.5 wt%) was added on top of each roof tile mixture

a jaw crusher (Retsch BB 200), and sieved at < 1.4 mm in order to have the same grain size distribution as the industrial blend. The sands (local and regional), the filler G from the roof tile blend, and the tailing material (SUL_PL_62_I) were fine enough to be integrated into the blends without mechanical pre-treatment.

For physical, mineralogical, and chemical characterization, the dried samples were homogenized, and a representative sample was ground and sieved at < 2 mm, < 250 µm, and < 200 µm, depending on the intended analysis.

For the environmental compliance tests (column leaching) performed on fired test specimens, pre-treatment of samples was done according to the CMA/5/B.3 method [31] and included crushing with a jaw crusher (Retsch BB 200) and sieving (95 wt% < 4 mm).

Characterization Methods

Moisture content was determined by drying samples at 105 °C. Specific surface area (SSA) was determined by methylene blue adsorption on powdered samples (< 250 µm). Grain size distribution analysis was performed on the pre-treated samples, after wet sieving (50 µm), splitting the samples in two fractions. The fraction < 50 µm was analyzed by a sedigraph machine (Micromeritics SediGraph 5100) based on the sedimentation method [32], while the fraction > 50 µm was dried and then sieved on a mechanical shaking column with sieves ranging from 1.4 to 0.09 mm (Retsch AS 200 control).

Mineralogical characterization of the tailing material was performed by X-ray powder diffraction (XRD) (Philips Analytical X-ray, model PW1830 generator with a PW3710 mpd control) on a powdered sample (< 200 µm) with CuKα radiation at 45 kV and 30 mA, and qualitative identification of the mineral phases was based on the Rietveld method [33] using the Profex software (version 3.14.3).

Total element concentrations were determined on the powdered samples (< 250 µm) by X-ray fluorescence (XRF) spectrometry (Panalytical Axios-Minerals, using superQ software with Omnian module) for major elements, and by inductively coupled plasma optical emission spectrometry (ICP-OES Varian Vista MPX), based on ISO 14869-1:2001 [34], for trace elements (mainly for Ba, Cr, Cu, Ni, Pb, and Zn). Total carbon and sulfur content were determined on powdered samples (< 250 µm) by a non-dispersive infrared (NDIR) analyzer (Leco SC632), based on the standard ISO 10694:1995 [35]. The gross loss on ignition (LOI) at 1000 °C of powdered samples (< 250 µm) was determined based on the standard NBN EN 15935:2012 [36].

Carbonate content, expressed as $CaCO_3$, was determined by titration of CO_2 from the decomposed carbonates of the powdered samples (< 250 µm) using a Mettler Toledo T70 and Phototrode DP5. Soluble sulfates (SO_4^{2-}) were measured for the powdered samples (< 250 µm, L/S = 3 l/kg) by ion chromatography (Metrohm 761 Compact IC), based on the standard NBN EN ISO 10304-1:2009 [37]. Only for the tailing sample, the L/S ratio was changed to 8.3 l/kg. Inductively coupled plasma optical emission spectrometry (ICP-OES Varian Vista MPX) was used to determine soluble cations (Ca^{2+}, Mg^{2+}, Na^{+} and K^{+}). For both analyses, unfired samples were prepared by refluxing with distilled

water for 6 h, while fired samples were shaken in distilled water for 1 h at 120 strokes/min.

The drying behavior (speed of weight loss, drying shrinkage, drying efflorescence, and appearance of cracks) of the wet test specimens was studied on lab scale and compared to the standard after being submitted to different drying programs, with different temperatures (°C) and relative humidity percentages (% RH) using a climate chamber (Vötsch VC3 4060 with S!MPATI® software). Other wet test pieces were dried in an industrial drier (60 h with 65 °C as maximum drying temperature) in the case of roof tile and block test pieces, or in a lab drier (12 h at 29 °C and 50% RH) in the case of paver test pieces. The drying shrinkage was measured and compared to the standard. The dried test pieces were then fired in electric lab kilns (Fours H&C SPRL, Type 25 and 100) at 985 °C and 1000 °C, at a speed of 90 °C/h and dwell time of 1 h, for the roof tile blends, at 965 °C, at a speed of 23 °C/h and dwell time of 30 min, for the block blends, and at 1130° C, at a speed of 90 °C/h and dwell time of 2 h for the paver blends. The firing shrinkage of all the fired test specimens was measured and compared to the standard. Firing color was visually compared to the standard.

Water absorption tests were performed on fired test specimens. For roof tiles, a progressive water immersion test (E_{prog}) and a full vacuum water immersion test ($E_{2.7kPa}$) are common, while for blocks and pavers, a 24 h water immersion test (E_{24h}) is the standard. The modulus of elasticity, *E*-modulus, was determined on the fired test specimens by using the software GENEMOD, as well as the dimensions (length, height and width), weight, and natural vibration (*R* value, µs). The natural vibration was measured with a non-destructive impulse excitation technique (ASTM E1876-15 standard) [38], using a J.W. Lemmens GrindoSonic machine, model MK5 Industrial. An in-house efflorescence test was performed on fired test specimens to assess their sensibility to efflorescence. Test pieces were laid horizontally (roof tiles) or vertically (blocks and pavers) in approximately 5 mm of distilled water. After 3 days, the test pieces were dried overnight in a ventilated stove at 50 °C (Heraeus UT 6060). This process was repeated 3 times, and lastly, the pieces were dried overnight in the same stove at 105 °C.

Environmental compliance tests were performed on the fired test specimens. The column leaching tests (L/S_{cum} = 10 l/kg, 7 fractions, 21 days) were performed on fired test specimens for roof tiles (985 °C), blocks (965 °C) and pavers (1130 °C). These tests were done according to method CMA/2/II/A.9.1 [27], based on the NEN 7373:2004 standard [39]. Element concentrations in the leachates were determined by ICP-OES (Agilent Technologies 5100), according to method CMA/2/I/B.1 [31].

Preparation of Ceramic Mixtures

For the preparation of the clay roof tile and block blends, all materials were mixed by hand and water was added to reach a good plasticity. After that, further homogenization was obtained by using a mechanical mixing machine. Finally, the mixtures were extruded (die 58 × 16 mm) under vacuum conditions, and 12 pieces per mix were cut at length of around 116 mm. The test pieces received a caliper marking (100 mm) in order to measure their drying and firing shrinkage. Drying was performed in an industrial dryer (see 'Characterization Methods'). The drying was followed by firing in electric lab kilns (see 'Characterization Methods').

For the clay paver blends, instead of extruding, test pieces were molded with a hand press (mold 110 × 55 × 20 mm). Twelve test pieces per mixture were prepared, and all of them received a caliper marking (100 mm). The produced test pieces were dried in a lab dryer (see 'Characterization Methods') and fired in an electric lab kiln (see 'Characterization Methods') (Fig. 1).

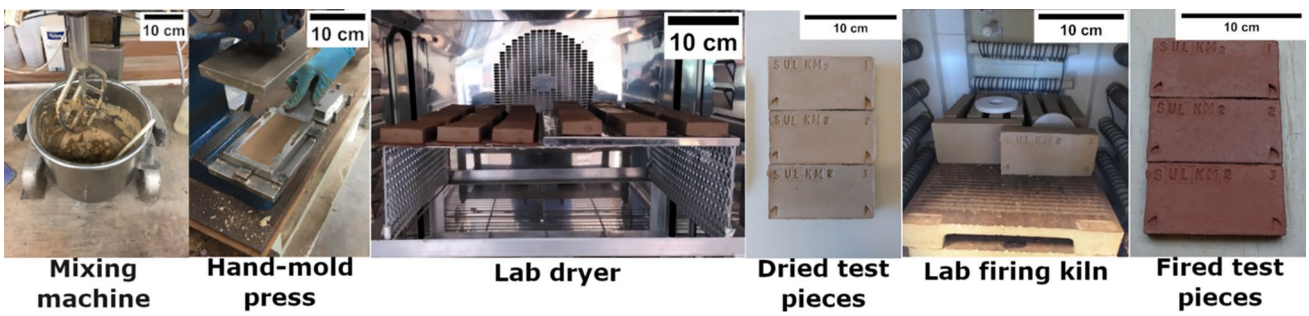

Fig. 1 Lab production of clay paver mixtures and test specimens

Results and Discussion

Characterization of the Materials

Plombières Tailing Material (SUL_PL_62_I)

Plombières tailing material is a clayey-silt material (86 wt% < 50 µm) with a SSA of 93 m^2/g. The tailing (pH 7.14) shows a low sulfur (0.01 wt% total S) and carbon (0.1 wt% total C) content, and only traces of heavy metals (23 mg/kg Cu, 30 mg/kg Pb, and 137 mg/kg Zn). The tailing material is poor in lime (0.07 wt% $CaCO_3$). The content of soluble sulfates is low (0.01 wt%). Compared to the clay materials used in the roof tile, block, and paver blends, the LOI of the tailing is low (3.3 wt%).

The major elemental composition (74 wt% SiO_2 and 12 wt% Al_2O_3) is in line with the qualitative XRD results, showing ceramic-friendly minerals as major mineral phases, such as quartz (SiO_2), phyllosilicates (e.g., muscovite ($KAl_2(AlSi_3O_{10})(OH)_2$), chlorite ($(Mg, Fe)_3(Si, Al)_4O_{10}(OH)_2{\cdot}(Mg, Fe)_3(OH)_6$), and feldspar (e.g., plagioclase ($NaAlSi_3O_8$ to $CaAl_2Si_2O_8$). The presence of an amorphous phase could be attributed to the presence of metallurgical slag in the tailings pond [28].

The environmental performance tests proved that the tailing material stays below the established guidance (total metal(loid)s concentration) and limit (total organic compound and leached metal concentrations) values, according to the Flemish environmental regulation on the sustainable management of material cycles and waste [40]. This means that it can be used in or as a non-shaped building material [26].

In summary, due to the low sulfur and metal(loid)s content, and the fact that it does not need any mechanical and/or (bio)chemical pre-treatment, the fine tailing material is a promising raw material for ceramics.

Company-Specific Materials

In the *clay roof tile* mixture with 20 wt% tailing material (SUL_PM_4), all four raw materials were partly replaced. Both clays (local and imported) are characterized by high < 2 µm fractions and SSA values (Table 2). The local clay has considerable amounts of total sulfur (0.6 wt%), carbon (0.5 wt%), and soluble sulfates (0.2 wt%). The high LOI values of both clays are linked to the clay mineral content and, in the case of the local clay, also to the total S and C content. The local sand is almost a pure quartz sand (96 wt% SiO_2) and can be considered as a fine sand (89 wt% < 200 µm). The imported filler G is a very fine material (76 wt% < 50 µm) with high lime content (10.4 wt% $CaCO_3$) (Table 2).

In the *clay block* mixtures, three raw materials were partly (local clay and imported filler R) or totally (regional sand) replaced by the tailing material. The local clay is the same as the one used for clay roof tiles. The imported filler R is a coarse material (66 wt% > 200 µm), containing some lime (1.6 wt% $CaCO_3$). The total sulfur content is mainly present in the form of soluble sulfates (0.1 wt%). The regional sand is a pure quartz sand (99.2 wt% SiO_2) and coarser (89 wt% > 200 µm) than the one used for the roof tile mixtures (Table 2).

Concerning the *clay paver* mixtures, the ready-for-use mixture, as received, was partly replaced by the tailing material (SUL_PL_62_I). The received paver mix is a fine material (83 wt% < 200 µm), with some lime (3.6 wt% $CaCO_3$) but very low total sulfur and soluble sulfates content (Table 2).

Characterization and Quality Assessment of Ceramic Blends

Clay Roof Tiles

All four unfired mixtures, the standard (SUL_PM_1), and those with 5 wt% (SUL_PM_2), 10 wt% (SUL_PM_3), and 20 wt% (SUL_PM_4) of the tailing material (SUL_PL_62_I) have similar physical properties, such as grain size distribution, SSA, and moisture content for a comparable plasticity (Supplementary Appendix A). Concerning the chemical properties of the unfired mixtures, the lime content ($CaCO_3$) slightly decreases with an increase of the tailing material due to the replacement of local clay and, especially, of the lime-rich imported filler G (Table 2) in the mix with 20 wt% of tailing material (SUL_PM_4). Major elemental composition of all unfired mixtures shows high silica (70 wt% SiO_2) and alumina (12 wt% Al_2O_3) content (Supplementary Appendix A). LOI values decrease along with the decrease in local and imported clay (Supplementary Appendix A). The high Ba content in all four unfired mixtures comes from the $BaCO_3$ addition. $BaCO_3$ prevents drying efflorescence as it reacts with the soluble sulfates, turning them into insoluble $BaSO_4$ [41]. All unfired mixtures present only traces of heavy metals, such as Cu, Zn, and Pb (Supplementary Appendix A).

After firing at 985 °C, all four fired mixtures show a decrease in total C (Supplementary Appendix A), as carbonates decompose and organic C burns away. The total S content remains stable or shows a slightly lower value when compared to the unfired mix (Supplementary Appendix A). This means that the CaO formed during firing, from the decomposition of lime, reacts with the SOx, from the decomposition of pyrite, to form $CaSO_4$ ($CaO + SO_2 + ½O_2 = CaSO_4$) [42]. This reaction explains the

Table 2 Physical and chemical characterization of Plombières tailing and replaced company-specific raw materials

Materials	1400–1000 µm (wt%)	1000–200 µm (wt%)	200–50 µm (wt%)	50–2 µm (wt%)	< 2 µm (wt%)	SSA (wt%)	$CaCO_3$ (wt%)	$CaO_{carbonates}$ (wt%)	$CO_{2carbonates}$ (wt%)	C_{total} (wt%)	$C_{organic}$ (wt%)
SUL_PL_62_I	3	3	8	47	39	93	0.1	0.04	0.03	0.1	0.1
Local clay	0	0	1	43	56	241	1.5	0.9	0.7	0.5	0.3
Imported clay	0	1	3	24	72	116	0.8	0.4	0.4	0.2	0.1
Local sand	0	11	85	4	0	23	0.1	0.04	0.03	0.02	0.01
Imported filler G	0	1	23	44	32	35	10.4	5.82	4.6	1.2	< LOD
Regional sand	0	89	11	0	0	23	0.1	0.04	0.03	0.01	0.001
Imported filler R	18	48	12	8	14	72	1.6	0.9	0.7	0.4	0.2
Paver mix	1	16	20	24	39	82	3.6	2.0	1.6	0.7	0.3
Materials	SiO_2 (wt%)	Al_2O_3 (wt%)	Fe_2O_3 (wt%)	TiO_2 (wt%)	CaO (wt%)	MgO (wt%)	Na_2O (wt%)	K_2O (wt%)	MnO (wt%)	LOI (wt%)	S_{total} (wt%)
SUL_PL_62_I	74.0	12.0	4.3	0.9	0.6	0.9	1.1	2.4	0.2	3.3	0.01
Local clay	60.9	15.7	6.7	0.9	1.0	2.1	0.5	3.2	< LOD	7.3	0.6
Imported clay	57.5	19.8	9.1	1.1	1.1	0.5	< LOD	2.5	< LOD	8.2	< LOD
Local sand	96.1	1.1	1.1	0.1	0.1	0.1	< LOD	0.6	< LOD	0.6	< LOD
Imported filler G	63.6	11.7	3.7	0.5	6.7	2.0	2.0	3.1	< LOD	6.1	< LOD
Regional sand	99.2	0.3	0.1	< LOD	< LOD	< LOD	< LOD	0.1	< LOD	0.2	< LOD
Imported filler R	58.1	21.1	6.4	1.0	0.7	1.8	0.6	3.9	0.01	5.9	0.03
Paver mix	68.0	13.0	5.5	1.1	3.3	< LOD	1.0	2.2	0.2	5.4	< LOD
Materials	Ba (mg/kg)	Cr (mg/kg)	Cu (mg/kg)	Ni (mg/kg)	Pb (mg/kg)	Zn (mg/kg)	Soluble SO_4^{2-} (mg/kg)	Soluble Ca^{2+} (mg/kg)	Soluble Mg^{2+} (mg/kg)	Soluble Na^+ (mg/kg)	Soluble K^+ (mg/kg)
SUL_PL_62_I	366	60	23	31	30	137	0.01	52	5	13	22
Local clay	290	120	21	53	19	94	0.2	353	48	579	509
Imported clay	302	164	39	83	27	78	0.05	354	2	48	169
Local sand	91	39	7	11	8	16	0.01	97	36	8	211
Imported filler G	250	76	13	35	18	56	0.03	168	1	96	129
Regional sand	43	2	5	1	7	7	0.01	22	3	23	19
Imported filler R	154	103	45	62	11	103	0.1	274	9	333	434
Paver mix	383	84	38	37	22	73	0.02	276	2	55	37

LOD limit of detection

presence of considerable amounts of $CaSO_4$, which when in contact with humidity can form gypsum [43]. At a firing temperature of 1000 °C, $CaSO_4$ starts to decompose. This results in lower total S and soluble sulfates content in the fired mixtures (Supplementary Appendix A).

All four mixtures, the standard and the three tailing-containing mixtures showed similar drying behavior. The drying shrinkage and water release of the three tailing-containing mixtures were always comparable to the standard, in all the tested drying programs from the lab climate chamber. Moreover, no cracks or drying efflorescence was visible on lab or industrial dried test pieces.

Replacing primary raw materials by tailing material may affect the ceramic product properties. Apart from small efflorescence stains (Fig. 2b, d), the fired test pieces with 5 wt% tailing material still show satisfying technical (Table 3) and chemical (Supplementary Appendix A) properties. However, the more clay (local or imported) is replaced by the clayey-silt tailing material (Table 2), the higher the porosity (water absorption) and the lower the strength (*E*-modulus). This is visible on the 10 and 20 wt% tailing mixtures (Table 3). The higher porosity of the fired test pieces, containing tailing material, is most probably the reason of the higher efflorescence stains on the fired bodies (Fig. 2b, d), despite their lower soluble sulfate content (Supplementary Appendix A). Although soluble sulfates decrease with an increase of the firing temperature (1000 °C), efflorescence stains are still visible on the fired bodies (Fig. 2d). The firing color of the three tailing-containing mixtures is always comparable with the standard for both firing temperatures, and a black core never occurred (Fig. 2a, c). In order to incorporate higher amounts of tailing material (10 and 20 wt%) in this particular roof tile mixture, higher replacement of local sand should be considered.

Clay Inner-Wall Blocks

All three unfired block mixtures, the standard mixture (SUL_ZM_1) and the mixtures with 10 wt% (SUL_ZM_2) and 20 wt% (SUL_ZM_3) of tailing material, have similar physical and chemical properties (Supplementary Appendix B). However, in SUL_ZM_3 mixture, with the highest addition of tailing material, there is a slight decrease of the 2 µm fraction, total C and S, and $CaCO_3$ content. This is the result of the partial replacement of local clay, richer in total C and S, and further decrease of imported filler R, coarser and richer in total C (Table 2). The three unfired mixtures have the same major element composition, with abundance of silica (58 wt% SiO_2) and alumina (16 wt% Al_2O_3), and low heavy metal (Cu, Zn, and Pb) content (Supplementary Appendix B).

The three fired block mixtures (965 °C) show, for the same reason as discussed in 'Clay Roof Tiles,' a decrease of total C when compared to the unfired mixtures (Supplementary Appendix B). The standard (SUL_ZM_1) and 10 wt% tailing mix (SUL_ZM_2) have similar values for the total C and S content, and soluble sulfates (Supplementary Appendix B). On the other hand, the mix with the highest tailing content (SUL_ZM_3) behaves different. It contains almost no total C, and soluble sulfates (and cations) are much lower than in the two other mixtures, as if less free CaO, K_2O, NaO_2, and MgO were available to react with SOx during firing.

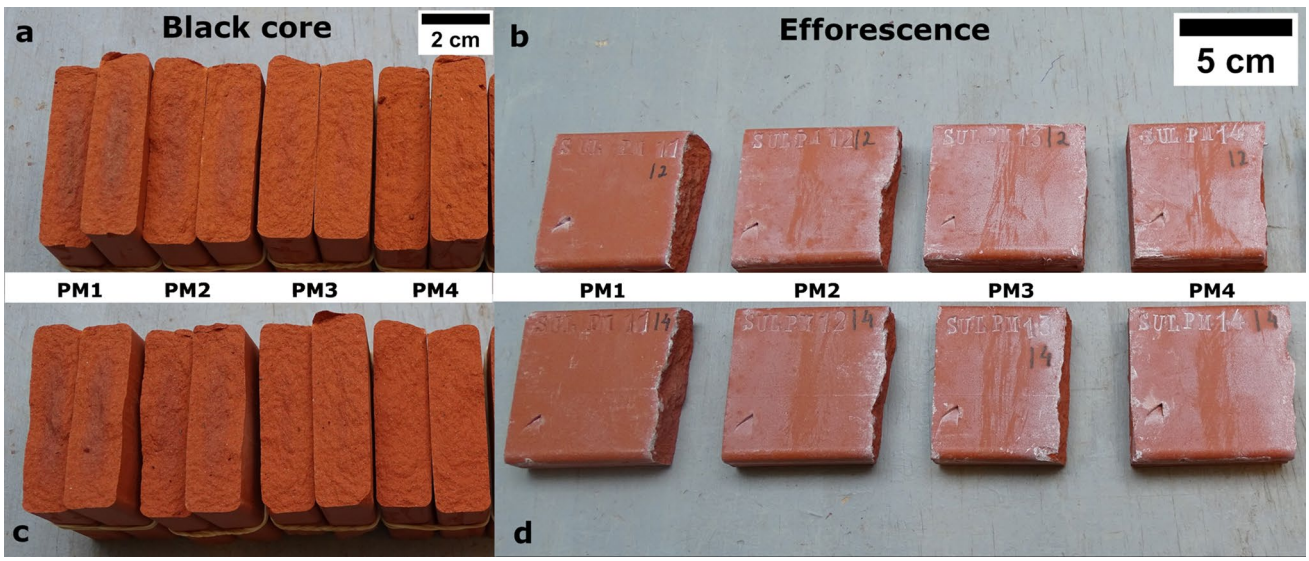

Fig. 2 Aesthetical properties of the roof tile mixtures fired at 985 °C (**a**, **b**) and 1000 °C (**c**, **d**)

Table 3 Technical properties of the fired ceramic mixtures

Roof tile mix	Firing shrinkage (%)		Water absorption (wt%)		Saturation level ($E_{prog}/E_{2.7kPa}$) (%)		*E*-modulus strength (GPa)	
	985 °C	1000 °C	E_{prog} 985 °C	E_{prog} 1000 °C	985 °C	1000 °C	985 °C	1000 °C
SUL_PM_1	1.6	2.0	7.2	6.2	71	66	18.0	19.8
SUL_PM_2	1.4	2.1	7.5	6.6	73	68	18.0	19.1
SUL_PM_3	1.6	2.2	8.0	7.1	74	70	16.5	18.1
SUL_PM_4	1.5	1.8	8.7	7.9	78	74	15.0	16.6
Block mix	Firing shrinkage (%)		Water absorption (wt%)		Saturation level ($E_{prog}/E_{2.7kPa}$) (%)		*E*-modulus strength (GPa)	
	965 °C		E_{24h} 965 °C		965 °C		965 °C	
SUL_ZM_1	1.0		10.5		NA		17.6	
SUL_ZM_2	1.2		10.5		NA		18.2	
SUL_ZM_3	1.2		12.6		NA		13.5	
Block mix	Firing shrinkage (%)		Water absorption (wt%)		Saturation level ($E_{prog}/E_{2.7kPa}$) (%)		*E*-modulus strength (GPa)	
	1130 °C		E_{24h} 1130 °C		1130 °C		1130 °C	
SUL_KM_1	3.8		3.0		NA		27.6	
SUL_KM_2	4.0		1.7		NA		28.6	
SUL_KM_3	4.2		1.9		NA		30.5	

NA not applicable

No difference in the drying behavior (drying shrinkage and water release) was observed between the standard and the two tailing-containing mixtures for all the tested drying programs in the lab climate chamber. No cracks or drying efflorescence were visible on lab or industrial dried test pieces.

The replacement of primary raw materials by tailing material in the block mixtures shows that as long as the tailing material replaces coarser materials (regional sand and imported filler R), the properties of the ceramic test pieces are satisfactory or even better than those of the standard. In fact, the 10 wt% tailing mix (SUL_ZM_2) shows the same water absorption and higher *E*-modulus strength (Table 3). The increase in strength can be linked to a more pronounced black core (Fig. 3a), which is the result of having a finer mixture (Supplementary Appendix B). Black core occurs when C from carbonaceous material is oxidized to COx, which can take oxygen from hematite (Fe_2O_3), creating a reducing atmosphere in the body and transforming hematite into magnetite (Fe_3O_4) ($Fe_2O_3 + CO = Fe_3O_4 + CO_2$), which results in the formation of a black core [42]. No difference in efflorescence was observed in the fired body with 10 wt% of the tailing material (SUL_ZM_2) when compared to the standard (Fig. 3b). Considering the 20 wt% tailing mixture (SUL_ZM_3), from the moment the fine plastic local clay is partly replaced (8 wt%) by the tailing material, the black core disappears (Fig. 3a), strength decreases and porosity increases substantially (Table 3). The absence of a black core is mainly linked to the decrease of the fine and plastic clay (local clay), thus, decreasing the < 2 µm fraction of the mixture, as well as linked to the slightly lower organic C content (Supplementary Appendix B). In this black core-free fired mixture, there is also a considerable decrease in soluble salt content (SO_4^{2-}, Ca^{2+}, Mg^{2+}, Na^+, and K^+) (Supplementary Appendix B). Nevertheless, due to a more open-body structure, soluble salts move easier to the surface through capillarity flow [44], resulting in more efflorescence. In order to incorporate a higher percentage of tailing material (20 wt%) in this company-specific block mixture, replacing less local clay and more regional sand and filler materials, should be considered.

Clay Pavers

Except for the slight decrease in lime ($CaCO_3$) content in the tailing-containing mixtures (SUL_KM_2 and SUL_KM_3), all the other physical and chemical properties are similar and comparable with the standard (SUL_KM_1). All three unfired mixtures have very low total S and soluble sulfates content (Supplementary Appendix C).

Compared to the unfired blends, the lab fired (1130 °C) mixtures show a considerable decrease in total C and in soluble sulfates content (Supplementary Appendix C).

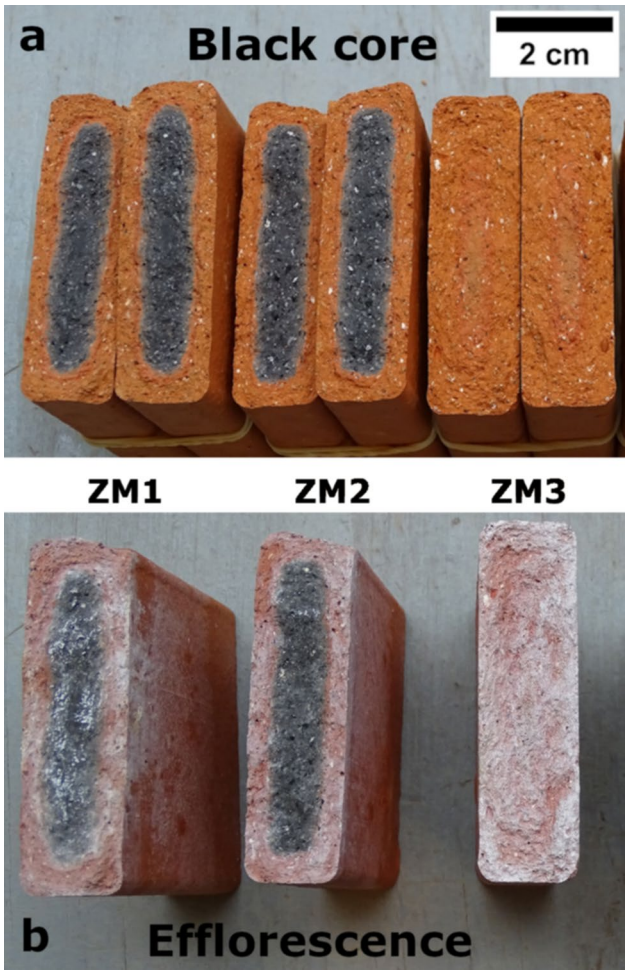

Fig. 3 Aesthetical properties of the block mixtures fired at 965 °C (**a**) black core, and (**b**) efflorescence

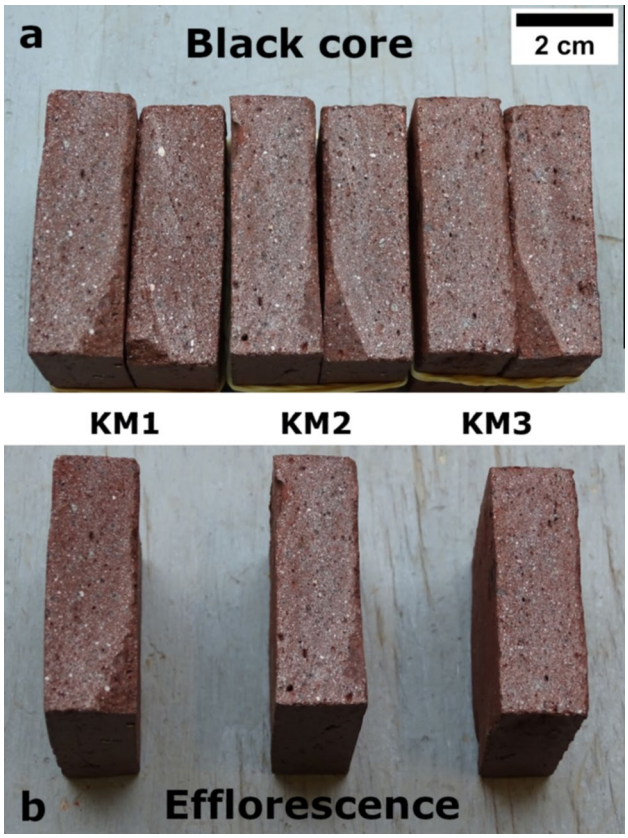

Fig. 4 Aesthetical properties of the paver mixtures fired at 1130 °C (**a**) black core and (**b**) efflorescence

The standard and the two tailing-containing paver mixtures show similar drying behavior for all the tested drying programs in the lab climate chamber. No cracks or drying efflorescence were visible on lab dried test pieces.

The paver mixtures containing 10 wt% (SUL_KM_2) and 20 wt% (SUL_KM_3) of tailing material presented satisfying technical properties, achieving lower water absorption and higher *E*-modulus strength when compared to the standard mix (Table 3), two important characteristics for the clay pavers as an outdoor floor application. The replacement of the ready-to-use paver mix by the fine tailing material (10 and 20 wt%) has slightly increased the silt (50–2 µm) and clay (< 2 µm) fractions of the paver test blends (Supplementary Appendix C), which seems to be enough to improve technical properties (Table 3). Concerning aesthetical properties, black core formation is not visible in any paver fired test piece (Fig. 4a) mainly due to the hand-molded shaping process (Fig. 1) that gives a more open structure to the test pieces, when compared to the extruded pieces, and also the low total C content and absence of S in the unfired mixtures (Supplementary Appendix C). Efflorescence ($CaSO_4$ formation) was not visible in the fired standard and tailing-containing mixtures (Fig. 4b), as almost no soluble salts were detected in these mixtures (Supplementary Appendix C) and due to the very low porosity (water absorption) of the fired test pieces.

Second Life Scenario for Building Ceramics

For the assessment of a 2nd life scenario where shaped building products can be demolished and recycled as aggregate materials, the standard mixtures and the 20 wt% tailing-containing mixtures were selected for the column leaching test according to CMA/2/II/A.9.1 [31]. Compared to the standard, the 20 wt% tailing mixtures for roof tiles (985 °C) and blocks (965 °C), showed a decrease in leachability of As, while for pavers (1130 °C), a slight increase in maximum leachability of As was visible (Table 4). To evaluate the pH-dependent leaching behavior (Fig. 5) the first eluate fraction (L/S = 0.1 l/kg) was omitted as it is often influenced by wash-off. For both roof tile mixtures, SUL_PM_1 ($R^2 = 0.9$) and SUL_PM_4 ($R^2 = 0.9$), As and

Table 4 Metal(loid) leaching from the fired ceramic mixtures (cumulative quantity release during column test)

Ceramic mixtures	pH[b]	Element concentration leached during column leaching test (Cumulative Release)[c] (mg/kg)						
		As	Cd	Cr	Cu	Ni	Pb	Zn
Limit values (VLAREMA, 2012)[a]		0.8	0.03	0.5	0.5	0.75	1.3	2.8
SUL_PM_1 (985 °C)	8.18	0.64	< LOD	0.18	0.001–0.03	0.01–0.03	< LOD	0.03
SUL_PM_4 (985 °C)	8.23	0.32–0.40	< LOD	0.27–0.32	< LOD	< LOD	< LOD	< LOD
SUL_ZM_1 (965 °C)	8.22	0.32	< LOD	0.12	< LOD	0.02–0.04	< LOD	0.02
SUL_ZM_3 (965 °C)	8.11	0.13–0.21	< LOD	0.18–0.23	< LOD	< LOD	< LOD	< LOD
SUL_KM_1 (1130 °C)	8.55	0.42	< LOD	0.002–0.10	0.002–0.10	< LOD	< LOD	< LOD
SUL_KM_3 (1130 °C)	8.63	0.63	< LOD	0.003–0.10	0.001–0.10	< LOD	< LOD	< LOD

LOD limit of detection

[a]Values according to the Flemish environmental regulations VLAREMA (2012) Annex 2.3.2.B

[b]pH calculated at L/S = 10

[c]According to method CMA/2/II/A.9.1 (CMA, 2020). Quantity release of an element in each mixture was calculated using the formula $U_i = (V_i \times c_i) \div m_0$, where i is the index of the eluate fraction, U_i is the release quantity of a component per quantity of sample in eluate fraction (mg/kg), V_i is the volume of the eluate fraction (l), c_i is the concentration of the component in the concerned eluate fraction (mg/l), and m_0 is the dry mass of the test portion in the column (kg). When concentration of a component (c_i) in one or more eluate fractions is below the limit of detection (< LOD), the upper limit of U_i must be calculated by making c_i equal to the limit of detection, and the lower limit of U_i must be calculated by making c_i equal to 0. For calculation of the cumulative quantity release (ΣU_i), the released quantities (U_i) were added up. For concentrations lower than the limit of detection, two calculations must be carried out to indicate the upper and lower limits of ΣU_i

Cr leaching are pH-dependent, while in both block mixtures, SUL_ZM_1 ($R^2 = 0.5$) and SUL_ZM_3 ($R^2 = 0.9$), only the leaching of Cr seems to be pH dependent (Fig. 5). For both paver mixtures, SUL_KM_1 ($R^2 = 1$) and SUL_KM_3 ($R^2 = 0.9$), only the leaching of As is pH dependent. The leaching of Cr is below the limit of detection for nearly all eluate fractions; therefore, a pH-dependent behavior cannot be established (Fig. 5). The pH-dependent leaching of As and Cr in clay roof tile and block mixtures, and of As in paver mixtures, shows that these elements are more mobile as pH rises [45]. Moreover, thermal treatment of ceramics can also play a role in the mobility of metal(loid)s due to the further decomposition of sulfides, if present, which often contain these hazardous elements [46]. No, Cd, and Pb were released from the tested ceramic mixtures during the column leaching tests. Nonetheless, it is noteworthy to say that leaching of elements from non-shaped materials is not only controlled by pH conditions but also by their buffer capacity, chemical speciation of elements, soluble salt and organic matter, redox potential, as well as physical factors, such as permeability, particle size, and porosity [47].

Regardless the leaching patterns, none of the assessed ceramic mixtures for roof tiles, blocks, and pavers were above the established leaching limits of the Flemish regulation [36] for As, Cd, Cr, Cu, Ni, Pb, and Zn (Table 4), which means that they can be recycled and used as non-shaped building materials (e.g., aggregates). Organic compounds and mercury (Hg), foreseen in the same regulation, were not analyzed on the selected samples as they were fired at high temperatures (≥ 965 °C), thus, normally, free of those.

Conclusions

This study investigated the replacement of primary raw materials in ceramic mixtures for roof tiles, blocks, and pavers by up to 20 wt% of Plombières mine tailing material, taking into account production parameters, product quality, and environmental performance.

Satisfying results for technical, aesthetical, and chemical properties were obtained for the roof tile blend with 5 wt%, the block blend with 10 wt%, and the two paver blends with 10 and 20 wt% of Plombières fine tailing material.

Compared to the standard, the roof tile blend with 5 wt% of tailing material showed similar technical and chemical properties, while efflorescence slightly increased. Concerning the block blends, the incorporation of 10 wt% improved E-modulus strength. Higher additions of tailing material in roof tiles (10 and 20 wt%) and blocks (20 wt%) resulted in an increase of water absorption, a decrease of E-modulus values, and more efflorescence, even though soluble salt content decreased. The replacement of the ready-to-use paver mix by 10 and 20 wt% of Plombières tailing improved product quality. Water absorption decreased while E-modulus increased. The clay pavers proved to be the most suitable ceramic product to incorporate higher amounts of this tailing material.

Considering a 2nd life scenario, where shaped building products are demolished and recycled as non-shaped building materials (e.g., aggregates), the clay roof tile, block, and paver test pieces with 20 wt% of tailing material, showed compliance with the Flemish environmental regulations.

In a raw-material-intensive industry, such as traditional ceramics, the replacement of primary raw materials by

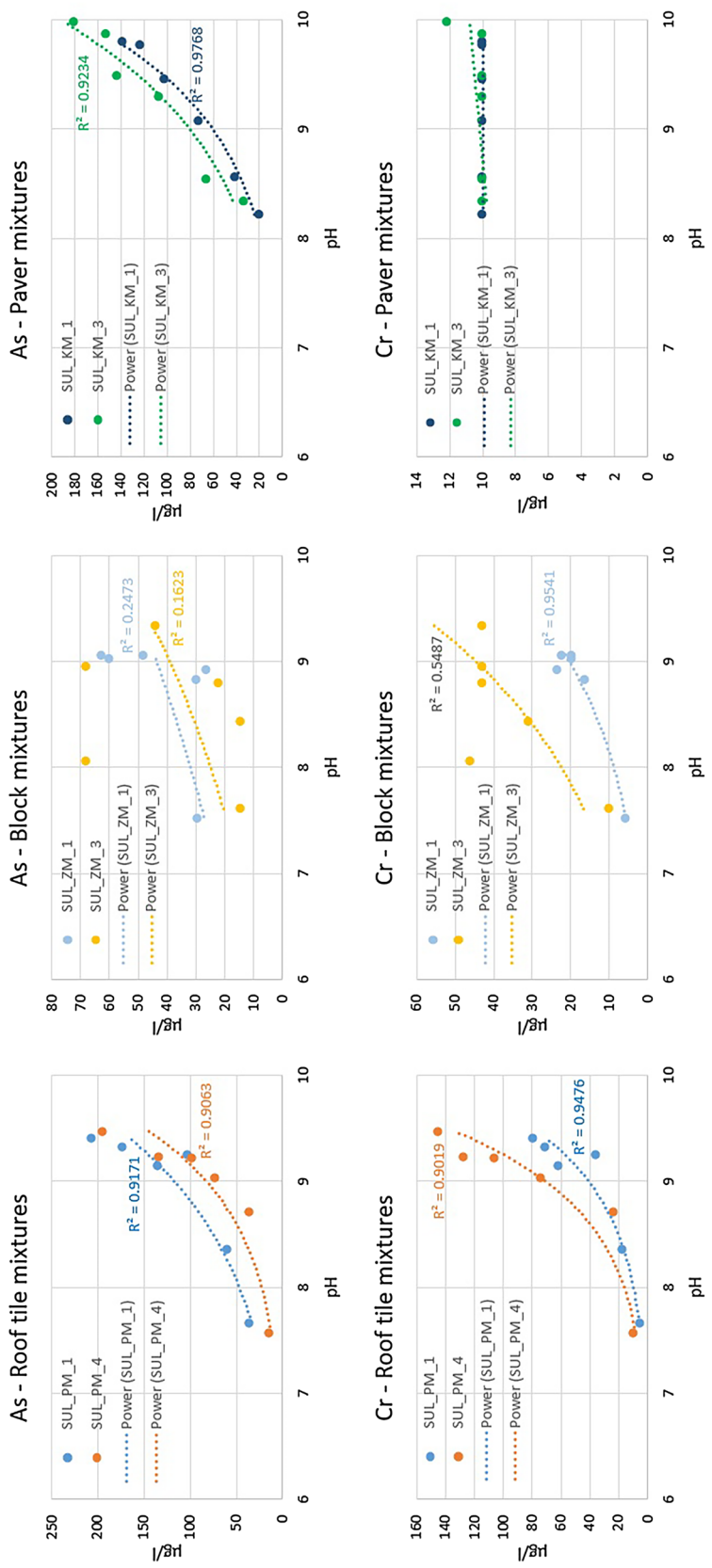

Fig. 5 Column leaching behavior of As and Cr in the selected roof tile (985 °C), block (965 °C), and paver (1130 °C) fired mixtures

alternative raw materials, such as mining waste, is essential for moderating the pressure on the exhaustive primary raw materials sector. Further investigation will focus on evaluating higher additions of Plombières tailing material (up to 40 wt%) in other ceramic product (facing bricks), by assessing technical and aesthetical properties, as well as the environmental performance (usage and 2nd life stages) and life-cycle assessment of the tailing-containing facing bricks.

Supplementary Information The online version contains supplementary material available at https://doi.org/10.1007/s40831-021-00442-3.

Acknowledgements Acknowledgements go to the staff of the Central Laboratory for Clay Roof Tiles (Kortrijk) and Central Laboratory for Facing Bricks (Beerse) from Wienerberger NV (Belgium), of the Department of Earth and Environmental Sciences (Leuven) from KU Leuven (Belgium), and of the Laboratory of Waste and Recycling Technologies (Mol) from VITO NV (Belgium), for their availability and assistance with the experimental work. We would like to thank Srećko Bevandić for the information and support provided concerning the location, sampling, and mineralogy of the case study tailings, and to Els Bulcke for the valuable input regarding the classification of the studied company-specific raw materials and for the environmental compliance interpretation of the tailing material. This study is part of the EU H2020 MSCA-ITN-ETN SULTAN project, aiming at the remediation and reprocessing of sulfidic mining waste sites. This project has received funding from the European Union's Framework Programme for Research and Innovation, Horizon 2020, under Grant Agreement No. 812580.

Declarations

Conflict of interest The authors declare that they have no known conflict of interest or personal relationships that could have appeared to influence the work reported in this original research paper.

References

1. Hudson-Edwards KA, Jamieson HE, Lottermoser BG (2011) Mine wastes: past, present. Future Elements 7(6):375–380. https://doi.org/10.2113/gselements.7.6.375
2. Szczepańska J, Twardowska I (2004) III.6 Mining waste. In: Twardowska I (ed) Solid waste: assessment, monitoring and remediation. Waste management series, vol 4. Elsevier, Amsterdam, pp 319–385. https://doi.org/10.1016/S0713-2743(04)80015-1
3. BRGM (Bureau de Recherches Géologiques et Minières) (2001) Management of mining, quarrying and ore-processing waste in the European Union, Study made for DG Environment, European Commission, December 2001. https://ec.europa.eu/environment/waste/studies/mining/0204finalreportbrgm.pdf
4. European Commission (2014) Commission Decision of 18 December 2014 amending Decision 2000/532/EC on the list of waste pursuant to Directive 2008/98/EC of the European Parliament and of the Council Text with EEA relevance. 2014/955/EU. Brussels. https://eur-lex.europa.eu/legal-content/EN/TXT/PDF/?uri=CELEX:32014D0955&from=EN
5. Lottermoser BG (2010) Sulfidic mine wastes. In: Lottermoser BG (ed) Mine wastes, 3rd edn. Springer, Berlin, Heidelberg, pp 43–117. https://doi.org/10.1007/978-3-642-12419-8_2
6. Moeng K (2018) Community perceptions on the health risks of acid mine drainage: the environmental justice struggles of communities near mining fields. Environ Dev Sustain 21:2619–2640. https://doi.org/10.1007/s10668-018-0149-4
7. Rotta LHS, Alcântara E, Park E, Negri RG, Lin YN, Bernardo N, Mendes TSG, Filho CRS (2020) The 2019 Brumadinho tailings dam collapse: possible cause and impacts of the worst human and environmental disaster in Brazil. Int J Appl Earth Obs Geoinf 90:102119. https://doi.org/10.1016/j.jag.2020.102119
8. Menezes RR, Santana LNL, Neves GA, Ferreira HC (2012) Recycling of mine waste as ceramic raw materials: an alternative to avoid environmental contamination. In: Srivastava J (ed) Environmental contamination, Chapter 11. InTech, London, pp 199–220. https://doi.org/10.5772/31913
9. Salinas-Rodríguez E, Flores-Badillo J, Hernández-Ávila J, Vargas-Ramírez M, Flores-Hernández JA, Rodríguez-Lugo V, Cerecedo-Sáenz E (2017) Design and production of a new construction material (bricks), using mining tailings. Int J Eng Sci Res Technolo 6(6):225–238. https://doi.org/10.5281/zenodo.809079
10. Zhang L (2013) Production of bricks from waste materials – a review. Constr Build Mater 47:643–655. https://doi.org/10.1016/j.conbuildmat.2013.05.043
11. Monteiro SN, Vieira CMF (2014) On the production of fired clay bricks from waste materials: a critical update. Constr Build Mater 68:599–610. https://doi.org/10.1016/j.conbuildmat.2014.07.006
12. Lamani SR, Aruna M, Vardhan H (2016) Utilisation of mine waste in construction industry—a critical review. Int J Earth Sci Eng, 9(1):182–195. https://idr.nitk.ac.in/jspui/handle/123456789/13699
13. Boltakova NV, Faseevaa GR, Kabirov RR, Nafikov RM, Zakharov YA (2017) Utilization of inorganic industrial wastes in producing construction ceramics. Review of Russian experience for the years 2000–2015. Waste Manage 60:230–246. https://doi.org/10.1016/j.wasman.2016.11.008
14. Murmu AL, Patel A (2018) Towards sustainable bricks production: an overview. Constr Build Mater 165:112–125. https://doi.org/10.1016/j.conbuildmat.2018.01.038
15. Menezes RR, Almeida RR, Santana LNL, Neves GA, Lira HL, Ferreira HC (2007) Analysis of the use of kaolin processing waste and granite sawing waste together for the production of ceramic bricks and roof tiles. Cerâmica 53:192–199. https://doi.org/10.1590/S0366-69132007000200014
16. Sultana S, Ahmed AN, Zaman MN, Rahman A, Biswas PK, Nandy PK (2015) Utilization of hard rock dust with red clay to produce roof tiles. J Asian Ceram Soc 3(1):22–26. https://doi.org/10.1016/j.jascer.2014.10.005
17. Flores-Badillo J, Ávila JH, Labra MP, Cardona FP, Santos JAO, Pineda NYT (2015) Developing alternative industrial materials from mining waste. In: Fergus JX, Mishra B, Anderson D, Sarver EA, Neelamenggham NR (eds) Engineering solutions for sustainability. Springer, Cham, pp 119–125. https://doi.org/10.1007/978-3-319-48138-8_11
18. Campos LFA, Menezes RR, Lisboa D, Santana LNL, Neves GA, Ferreira HC (2007) Experimental design to maximize the waste content in ceramic bricks and tiles. Cerâmica 53:373–380. https://doi.org/10.1590/S0366-69132007000400007
19. Abi E, Oruç F, Sabah E (2011) Utilization of waste clay from coal preparation tailings for brick production. J Ore Dress 13(25): 22–32. https://www.researchgate.net/publication/262179899_Utilization_of_Waste_Clay_from_Coal_Preparation_Tailings_for_Brick_Production
20. Cerqueira NA, Choe D, Alexandre J, Azevedo ARG, Xavier CG, Souza VB (2016) Properties of clay for ceramics with rock waste for production structural block by pressing and firing. In: Ikhmayies SJ et al (eds) Characterization of minerals, metals, and materials. Springer, Cham, pp 653–659. https://doi.org/10.1007/978-3-319-48210-1_82
21. Amaral LF, Carvalho JPRG, Silva BM, Delaqua GCG, Monteiro SN, Vieira CMF (2019) Development of ceramic paver with

ornamental rock waste. J Market Res 8(1):599–608. https://doi.org/10.1016/j.jmrt.2018.05.009
22. Lavrinenko AA, Svechnikova NY, Konovnitsyna NS, Igumensheva EA, Kuklina OV, Khasanzyanova AI (2018) Utilization of bituminous coal flotation wastes in the manufacture of ceramic brick. Solid Fuel Chem 52:406–410. https://doi.org/10.3103/S0361521918060083
23. Mendes BC, Pedroti LG, Alvarenga RCSS, Fontes MPF, Drumond PC, Pacheco AA, Lopes MMS, Azevedo ARG (2019) Effect of the incorporation of iron ore tailings on the properties of clay bricks. In: Li B et al (eds) Characterization of minerals, metals, and materials. Springer, Cham, pp 617–627. https://doi.org/10.1007/978-3-030-05749-7_61
24. Liu T, Xie Y, Guo X, Zhang J, Zhu L, Luo Z, Tang Y, Lu A (2021) The role and stabilization behavior of heavy metal ions in eco-friendly porous semi-vitrified ceramics for construction application. J Clean Prod 292:125855. https://doi.org/10.1016/j.jclepro.2021.125855
25. Bohn BP, Mühlen CV, Pedrotti MF, Zimmer A (2021) A novel method to produce a ceramic paver recycling waste glass. Clean Eng Technol 2:100043. https://doi.org/10.1016/j.clet.2021.100043
26. Veiga Simão F, Chambart H, Vandemeulebroeke L, Cappuyns V (2021) Incorporation of sulphidic mining waste material in ceramic roof tiles and blocks. J Geochem Explor. https://doi.org/10.1016/j.gexplo.2021.106741
27. Dejonghe L, Ladeuze F, Jans D (1993) Atlas des gisements plombo-zincifères du Synclinorium de Verviers (Est de la Belgique). Mémoire Service géologique de Belgique 33:1–148. https://difusion.ulb.ac.be/vufind/Record/ULB-DIPOT:oai:dipot.ulb.ac.be:2013/154131/Holdings
28. Helser J, Cappuyns V (2021) Trace elements leaching from Pb–Zn mine waste (Plombières, Belgium) and environmental implications. J Geochem Explor 220:106659. https://doi.org/10.1016/j.gexplo.2020.106659
29. Kucha H, Martens A, Ottenburgs R, De Vos W, Viaene W (1996) Primary minerals of Zn–Pb mining and metallurgical dumps and their environmental behavior at Plombières, Belgium. Environ Geol 27:1–15. https://doi.org/10.1007/BF00770598
30. Bevandić S, Blannin R, Vander Auwera J, Delmelle N, Caterina D, Nguyen F, Muchez P (2021) Geochemical and mineralogical characterisation of historic Zn–Pb mine waste, Plombières, East Belgium. Minerals 11(1):28. https://doi.org/10.3390/min11010028
31. CMA (2020) Compendium for sampling and analyses of waste and soil. Flemish Environmental Legislation. Ministerial approved version of December 16, 2020. https://emis.vito.be/nl/erkende-laboratoria/bodem-en-afvalstoffen-ovam/compendium-cma
32. Pye K, Blott SJ (2004) Particle size analysis of sediments, soils and related particulate materials for forensic purposes using laser granulometry. Forensic Sci Int 144:19–27. https://doi.org/10.1016/j.forsciint.2004.02.028
33. Rietveld HM (1969) A profile refinement method for nuclear and magnetic structures. J Appl Cryst 2:65–71. https://doi.org/10.1107/S0021889869006558
34. ISO 14869-1:2001. Soil quality—dissolution for the determination of total element content—Part 1: Dissolution with hydrofluoric and perchloric acids. https://www.iso.org/standard/28454.html
35. ISO 10694:1995. Soil quality—Determination of organic and total carbon after dry combustion (elementary analysis). https://www.iso.org/standard/18782.html
36. NBN EN 15935:2012. Sludge, treated biological waste, soil and waste—determination of the loss on ignition. https://www.nbn.be/shop/en/standard/nbn-en-15935-2012~466156/
37. NBN EN ISO 10304-:2009. Water quality—determination of dissolved anions by liquid chromatography of ions—Part 1: Determination of bromide, chloride, fluoride, nitrate, nitrite, phosphate and sulfate (ISO 10304-1:2007)(+ AC:2012). https://www.nbn.be/shop/en/standard/nbn-en-iso-10304-1-2009~327029/
38. ASTM E1876-15. Standard test method for dynamic Young's modulus, shear modulus, and poisson's ratio by impulse excitation of vibration. https://www.astm.org/Standards/E1876.htm
39. NEN 7373:2004. Leaching characteristics—determination of the leaching of inorganic components from granular materials with a column test—Solid earthy and stony materials. https://www.nen.nl/NEN-Shop-2/Standard/NEN-73732004-nl.htm
40. VLAREMA (2012) Decree of the Flemish Government establishing the Flemish regulations concerning the sustainable management of material cycles and waste. Last modified December 7, 2019. https://navigator.emis.vito.be/mijn-navigator?woId=43991&woLang=nl
41. Andrés A, Díaz MC, Coz A, Abellán MJ, Viguri JR (2009) Physicochemical characterisation of bricks all through the manufacture process in relation to efflorescence salts. J Eur Ceram Soc 29(10):1869–1877. https://doi.org/10.1016/j.jeurceramsoc.2008.11.015
42. Gredmaier L, Banks CJ, Pearce RB (2011) Calcium and sulphur distribution in fired clay brick in the presence of a black reduction core using micro X-ray fluorescence mapping. Constr Build Mater 25(12):4477–4486. https://doi.org/10.1016/j.conbuildmat.2011.03.054
43. Chwast J, Todorović J, H., Elsen, J., (2015) Gypsum efflorescence on clay brick masonry: field survey and literature study. Constr Build Mater 85:57–64. https://doi.org/10.1016/j.conbuildmat.2015.02.094
44. Ribeiro AG, Silva FAN, Azevedo AC, Lopes FAF, Delgado JMPQ (2020) The effect of soluble mineral salts in ceramic brick masonry. Int J Civ Eng 18:685–699. https://doi.org/10.1007/s40999-020-00502-x
45. Mitchell K, Moreno-Jimenez E, Jones R, Zheng L, Trakal L, Hough R, Beesley L (2020) Mobility of arsenic, chromium and copper arising from soil application of stabilised aggregates made from contaminated wood ash. J Hazard Mater 393:122479. https://doi.org/10.1016/j.jhazmat.2020.122479
46. Belmonte LJ, Ottosen LM, Kirkelund GM, Jensen PE, Vestbø AP (2018) Screening of heavy metal containing waste types for use as raw material in Arctic clay-based bricks. Environ Sci Pollut Res 25:32831–32843. https://doi.org/10.1007/s11356-016-8040-z
47. Van der Sloot HA, Dijkstra JJ (2004) Development of horizontally standardized leaching tests for construction materials: a material or release based approach? Identical leaching mechanisms for different materials. Technical Report no. ECN-C-04-060. https://doi.org/10.13140/rg.2.2.11986.76486